ISSN 2176-5480

22nd International Congress of Mechanical Engineering (COBEM 2013)
November 3-7, 2013, Ribeirão Preto, SP, Brazil

A MIXED CONVECTION STUDY IN A VENTILATED SQUARE CAVITY WITH AN INNER HOT BODY COOLED BY NANOFLUID

Paulo Mohallem Guimarães
Universidade Federal de Itajubá – Campus Itabira
pauloguimaraes@unifei.edu.br
Tamara Louzada
Universidade Federal de Itajubá – Campus Itabira
tamara@unifei.edu.br
Genésio José Menon
Universidade Federal de Itajubá – Campus Itajubá
genesio@unifei.edu.br

Abstract. *Heat transfer study is conducted inside a square ventilated cavity with a heat source placed at its center. The work fluid is a Cu/water nanofluid considering two nanoparticle concentrations. Reynolds number is varied from 50 to 500 and the Grashof number from 10^3 to 10^5. The inlet is in the opposite side of the outlet favoring buoyancy forces in the upward direction. Although the forced velocities go from bottom to top in the ascending direction inside the cavity, this work presents a curious result when the Reynolds number is increased by keeping the Grashof number constant. One should expect from this, that is, by increasing Reynolds number that heat transfer should increase. Nevertheless, the opposite happened. As Re increases, so do the strength and size of the recirculation that appears, and hence the fluid is stuck around the heated source and therefore weakening heat transfer. In general, the nanoparticle concentration effect of heat transfer enhancement is the order of 4% for concentrations of 0 (pure water) and 1%.*

Keywords: *mixed convection, nanofluid, ventilated cavity*

1. INTRODUCTION

The use of nanofluids in heat exchangers is still object of great interest once the thermophysical properties of their metal nanoparticles have high thermal conductivity. The use of this kind of fluid may allow manufacturing of more compact equipments and lower temperatures on heated surfaces to be cooled.

An interesting study was reported on the fluid flow and heat transfer characteristics associated with cooling an in-line array of discrete protruding heated blocks in a channel by using a single laminar slot air jet (Arquis et al., 2007). Numerical experiments were carried out for different values of jet Reynolds number, channel height, slot width, spacing between blocks, block height, and block thermal conductivity. The effects of variation of these parameters were detailed to illustrate important fundamental and practical results that are relevant to the thermal management of electronic packages. In general, the effective cooling of blocks was observed to increase with the increase of Reynolds number and the decrease of channel height. Circulation cells that may appear on the top surface of the downstream blocks were shown to decrease the value of Nusselt number for these blocks. The values of surface averaged Nusselt number attained their maximum at the block just underneath the impinging air jet, decreased for the downstream blocks, and approximately reached a constant value after the third block.

A numerical study (Madhusudhana & Narasimham, 2007) was carried out on conjugate mixed convection arising from protruding heat generating ribs attached to substrates forming a series of vertical parallel plate channels. A channel with periodic boundary conditions in the transverse direction was considered for analysis where identical disposition and heat generation of the ribs on each board were assumed. The governing equations were discretized using a control volume approach on a staggered mesh and a pressure correction method was employed for the pressure–velocity coupling. The solid regions were considered as fluid regions with infinite viscosity; and the thermal coupling between the solid and fluid regions was taken into account by the harmonic thermal conductivity method. Parametric studies were performed by varying the heat generation based Grashof number in the range 10^4–10^7 and the fan velocity was based on Reynolds number in the range 0–1500, with air as the working fluid. In pure natural convection, the induced mass flow rate varied at 0.44 power of Grashof number. The heat transferred to the working fluid via substrate heat conduction was found to account for 41–47% of the heat removal from the ribs.

Shahi et al. (2010) investigated the mixed convection flows through a copper‐water nanofluid in a square cavity with inlet and outlet ports. Buoyancy forces were that feature natural convection were attained by heating from the constant flux heat source located at the bottom wall and by cooling from the inlet flow. The governing equations were approximated by using the finite volume approach, using SIMPLE algorithm on the collocated arrangement. The study was carried out for the Reynolds number raging from 50 to 1000, with Richardson numbers from 0 to 10. The nanoparticle concentration was ranged from 0 to 0.05. The thermal conductivity and effective viscosity of nanofluid were calculated by Patel and Brinkman (1952) models, respectively. Results were presented in the form of streamlines, isotherms, average Nusselt number and average bulk temperature. In addition, the effects of solid volume fraction of

ISSN 2176-5480

nanofluids on the hydrodynamic and thermal characteristics were studied. The results indicated that increase in solid concentration led to increase in the average Nusselt number at the heat source surface and to decrease in the average bulk temperature.

Nassan et al. (2010) investigated the heat transfer in a square cross-section cupric duct in laminar flow under uniform heat flux by comparing heat exchange characteristics of Al_2O_3/water and CuO/water nanofluids. Sometimes because of pressure drop limitations, the need for noncircular ducts appeared and a testing facility was constructed for this purpose. Experimental studies were carried out being that those nanofluids had different nanoparticle concentrations. Distilled water was the base fluid to compose the nanofluids. The results showed that a significant heat transfer enhancement was achieved by both nanofluids compared with the case when pure water was used as the work fluid. Nevertheless, nanofluid with monoxide of copper showed better heat transfer augmentation compared with nanofluid with alumina through the square cross-section duct.

Rostamani et al. (2010) studied the turbulent flow of nanofluids with different volume concentrations of nanoparticles flowing through a two-dimensional duct under constant heat flux condition using numerical procedures. The nanofluids considered are mixtures of copper oxide (CuO), alumina (Al_2O_3) and oxide titanium (TiO_2) nanoparticles and water as the base fluid. All the thermophysical properties of nanofluids are temperature-dependent. The viscosity of nanofluids is obtained on basis of experimental data. The predicted Nusselt numbers exhibit good agreement with Gnielinski's correlation. The results show that by increasing the volume concentration, the wall shear stress and heat transfer rates increase. For a constant volume concentration and Reynolds number, the effect of CuO nanoparticles to enhance the Nusselt number is better than Al_2O_3 and TiO_2 nanoparticles.

Lotfi et al. (2010) conducted a study on forced convection in horizontal tubes with flow of a nanofluid having water as its base-fluid and Al_2O_3 as its nanoparticles. Results were validated with existing well established correlations in literature. Two-phase Eulerian model was implemented in order to study such a flow field. A single-phase model and two-phase mixture model formulations were also used for comparison. The comparison of calculated results with experimental values showed that the mixture model was more accurate. It was showed that the single-phase model and the two-phase Eulerian model underestimate the heat transfer.

Jung et al. (2009) studied the nanofluid convective heat transfer coefficient and friction factor behavior in rectangular microchannels. A microsystem consisting of a single microchannel on one side, and two localized heaters and five polysilicon temperature sensors along the channel on the other side were fabricated. Aluminum dioxide (Al_2O_3) with diameter of 170 nm nanofluids with various particle volume fractions were used. The convective heat transfer coefficient of the Al_2O_3 nanofluid in laminar flow regime was measured to be increased up to 32% compared to the distilled water at a volume fraction of 1.8 volume percent without major friction loss. The Nusselt number increased as Reynolds number went up in laminar flow regime. The Nusselt number, which was less than 0.5, was successfully correlated with Reynolds number and Prandtl number based on the thermal conductivity of nanofluids.

Arefmanesh and Mahmood (2001) analyzed the laminar mixed convection fluid flow and heat transfer in a square cavity regarding the effects of uncertainties in the effective dynamic viscosity of Al_2O_3–water nanofluid. The left and right vertical walls of the enclosure as well as its horizontal top wall were cooled at a constant temperature. The horizontal bottom wall of the cavity, which moves in its own plane from left to right with a constant speed, was kept at a constant heating temperature. The governing equations written in terms of the primitive variables were numerically approximated by using the finite volume method. Two different models proposed in the literature were considered for the effective dynamic viscosity of the nanofluid. A parametric study was performed incorporating the two viscosity formulas, and the effects of the Richardson number and the volume fraction of the nanoparticles on the velocity and temperature fields inside the enclosure were investigated. The results showed that there were significant differences between heat transfer enhancements in the cavity for the two viscosity models. In addition to this, the average Nusselt number of the hot wall generally increased as the nanoparticle concentration increased for both viscosity models.

2. PROBLEM DESCRIPTION

The goal of the present work is to study numerically the laminar mixed convection inside a square ventilated cavity with a square heat source. The flow enters in the lower part and exits in the upper part of the vertical walls of the cavity. All walls are thermally isolated and have no-slip condition. The heat source has a constant and uniform heat flux. The nanofluid is composed of water (base-fluid and Prandtl number Pr = 6.2) and copper nanoparticles. The nanofluid enters the cavity at constant velocity and low temperature and exits under symmetry conditions related to the Y-direction. The nanoparticle concentration is 1% due to the thermophysical property correlations applied here. Figure 1 depicts the problem geometry and boundary conditions. U and V are the dimensionless velocities, W is the cavity width, H is the cavity height, θ is the dimensionless temperature, and ρ_{nf}, μ_{nf}, and k_{nf} are the density, absolute viscosity and thermal conductivity of the nanofluid, respectively. These dimensionless variables and thermophysical parameters are going to be formally introduced later on.

ISSN 2176-5480

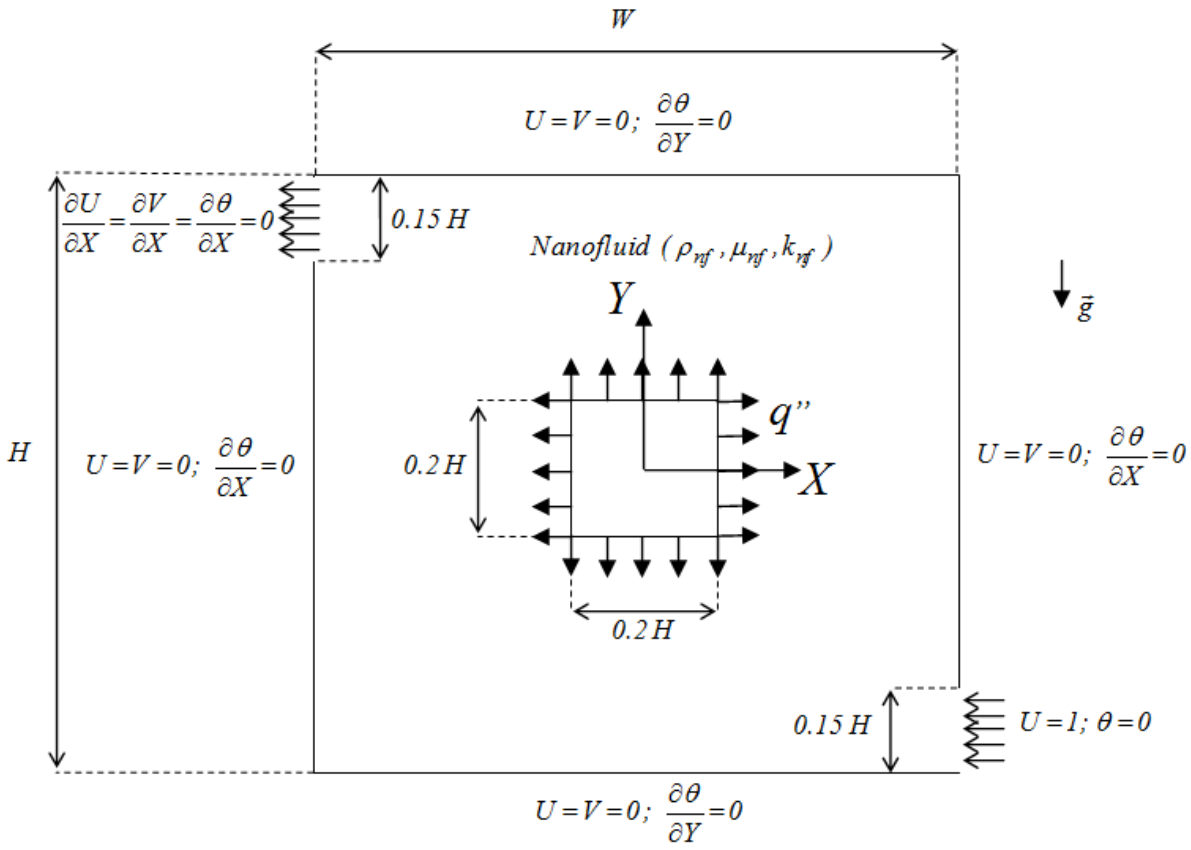

Figure 1 – Geometry and boundary conditions.

The problem governing equations are as follows:

Mass conservation

$$\frac{\partial u}{\partial x}+\frac{\partial v}{\partial y}+\frac{\partial w}{\partial z}=0 \tag{1}$$

Momentum Conservation

$$u\frac{\partial u}{\partial x}+v\frac{\partial u}{\partial y}+v\frac{\partial u}{\partial z}=\frac{1}{\rho_{nf}}\left[-\frac{\partial p}{\partial x}+\mu_{nf}\left(\frac{\partial^2 u}{\partial x^2}+\frac{\partial^2 u}{\partial y^2}+\frac{\partial^2 u}{\partial z^2}\right)\right] \tag{2}$$

$$u\frac{\partial v}{\partial x}+v\frac{\partial v}{\partial y}+w\frac{\partial v}{\partial z}=\frac{1}{\rho_{nf}}\left[-\frac{\partial p}{\partial y}+\mu_{nf}\left(\frac{\partial^2 v}{\partial x^2}+\frac{\partial^2 v}{\partial y^2}+\frac{\partial^2 v}{\partial z^2}\right)\right]+\left[\left(\rho\beta\right)_{nf}\left(T-T_c\right)\right]g \tag{3}$$

Energy conservation

$$u\frac{\partial T}{\partial x}+v\frac{\partial T}{\partial y}+w\frac{\partial T}{\partial z}=\alpha_{nf}\left(\frac{\partial^2 T}{\partial x^2}+\frac{\partial^2 T}{\partial y^2}+\frac{\partial^2 T}{\partial z^2}\right) \tag{5}$$

where the nanofluid effective density ρ_{nf} and the nanofluid thermal difussivity α_{nf} are:

$$\rho_{nf}=\left(1-\phi\right)\rho_f+\phi\rho_p \tag{6}$$

$$\alpha_{nf}=k_{nf}\Big/\left(\rho C_p\right)_{nf} \tag{7}$$

and Ø is the solid volume fraction of the nanoparticles. The subscripts f and p stand for fluid and particles, respectively. The nanoparticle, which will be considered in this study, is Copper (Cu). The base fluid is water with Prandtl number

ISSN 2176-5480

(Pr) equal to 6.2. Table 1 gives the thermophysical properties of water and nanoparticles according to Oztop and Abu-Nada (2008):

The heat capacitance (ρC_p) nf and the thermal expansion $(\rho\beta)$ nf of the nanofluid are written as:

$$\left(\rho C_p\right)_{nf} = (1-\phi)\left(\rho C_p\right)_f + \phi\left(\rho C_p\right)_p \tag{8}$$

$$\left(\rho\beta\right)_{nf} = (1-\phi)\left(\rho\beta\right)_f + \phi\left(\rho\beta\right)_p \tag{9}$$

The effective dynamic viscosity μ_{nf} of the nanofluid (Brinkman (1952)) is:

$$\mu_{nf} = \frac{\mu_f}{(1-\phi)^{2.5}} \tag{10}$$

The thermal conductivity k_{nf} in Eq. (6), for spherical particles and based on Maxwell –Garnett's model (1904), is:

$$k_{nf} = k_f \left[\frac{\left(k_p + 2k_f\right) - 2\phi\left(k_f - k_p\right)}{\left(k_p + 2k_f\right) + \phi\left(k_f - k_p\right)} \right] \tag{11}$$

where k_p is the thermal conductivity addressed to nanoparticle (Copper), and k_f is the thermal conductivity addressed to pure fluid (water). The Maxwell-Garnett's model has been cited by other authors such as Aminossadati and Ghasemi (2009), Ho et al. (2008) and Oztop and Abu-Nada (2008).

Table 1. Thermophysical properties of the nanoparticle and base-fluid

Thermophysical properties	Fluid phase (water)	*Cu*
Cp (J/kgK)	4179	385
ρ (kg/m³)	997.1	8933
K (W/mK)	0.613	400
β x 10⁻⁵ (1/K)	21	1.67

The dimensionless parameters are:

$$X = \frac{x}{H};\ Y = \frac{y}{H};\ U = \frac{u}{u_0};\ V = \frac{v}{u_0};\ P = \frac{p}{\rho_{nf} u_0};\ \theta = \frac{(T - T_c)}{(\Delta T)};\ Gr = \frac{g\beta_f H^3 \Delta T}{{\nu_f}^2};\ \Delta T = \frac{q'' H}{k_f};\ Pr = \frac{\nu_f}{\alpha_f};\ Ri = \frac{Gr}{Re^2};\ Re = \frac{u_o H}{\mu_f} \tag{12}$$

where: u and v – dimensional velocities, U and V – dimensionless velocities, p – dimensional pressure, P-dimensionless pressure, T – dimensional temperature, θ – dimensionless temperature, Gr – Grashof number, Pr – Prandtl number, Ri – Richardson number, ν – kinematics viscosity, α – thermal diffusivity, Re – Reynolds number.

Substituting (12) into (2) to (4), the final form the conservation equations are:

$$\frac{\partial U}{\partial X} + \frac{\partial V}{\partial Y} = 0 \tag{13}$$

$$U\frac{\partial U}{\partial X} + V\frac{\partial U}{\partial Y} = -\frac{\partial P}{\partial X} + \frac{1}{Re}\frac{\mu_{eff}}{\nu_f \rho_{nf}}\left(\frac{\partial^2 U}{\partial X^2} + \frac{\partial^2 U}{\partial Y^2}\right) \tag{14}$$

ISSN 2176-5480

$$U\frac{\partial V}{\partial X}+V\frac{\partial V}{\partial Y}=-\frac{\partial P}{\partial Y}+\frac{1}{Re}\frac{\mu_{eff}}{\nu_f\rho_{nf}}\left(\frac{\partial^2 V}{\partial X^2}+\frac{\partial^2 V}{\partial Y^2}\right)+\frac{(\rho\beta)_{nf}}{\rho_{nf}\beta_f}Ri\ \theta \tag{15}$$

$$U\frac{\partial \theta}{\partial X}+V\frac{\partial \theta}{\partial Y}=\frac{\alpha_{nf}}{\alpha f}\frac{1}{Pr\,Re}\left(\frac{\partial^2 \theta}{\partial X^2}+\frac{\partial^2 \theta}{\partial Y^2}\right) \tag{16}$$

The local Nusselt number on a certain surface is given by:

$$Nu^*_{hs}=\frac{hL}{k_f} \tag{17}$$

where h is the heat transfer coefficient:

$$h=\frac{q''}{T_s-T_c} \tag{18}$$

Substituting appropriate parameters from (12) and (18) into (17) yields the local Nusselt number:

$$Nu^*_{hs}(X,Y)=\left.\frac{1}{\theta(X,Y)}\right|_{hs} \tag{19}$$

where the subscript hs stands for the heater surface. Being that S is the surface length on where Nu^*_{hs} is integrated, the average Nusselt number is then calculated by:

$$Nu_{hs}(X,Y)=\frac{1}{S}\int_{hs}Nu^*_{hs} \tag{20}$$

3. NUMERICAL PROCEDURE AND CODE VALIDATION

Equations (13) to (16) are approximated by the finite element method with Petrov-Galerkin weighting on the convective terms and the pressure terms are approximated by a penalty technique with the penalty parameter equal to 10^9. These techniques will be omitted here for a space matter. The numerical method is implemented by using Fortran computational language. The code is thoroughly validated. First validation is carried out by comparing the average Nusselt number along the hot wall, the maximum velocities in the X and Y directions and their respective positions at Y and X axes, for Ra equal to 10^3, 10^4, 10^5 and 10^6. However, only comparisons for Ra equal to 10^3 and 10^6 and shown in Table 2. Air is the work fluid with Pr = 0.7. It consists of a benchmark problem in which a square differentially heated cavity is studied where the vertical wall temperatures are uniform and equal to 0 (cold wall) and 1 (hot wall). Excellent agreement is achieved.

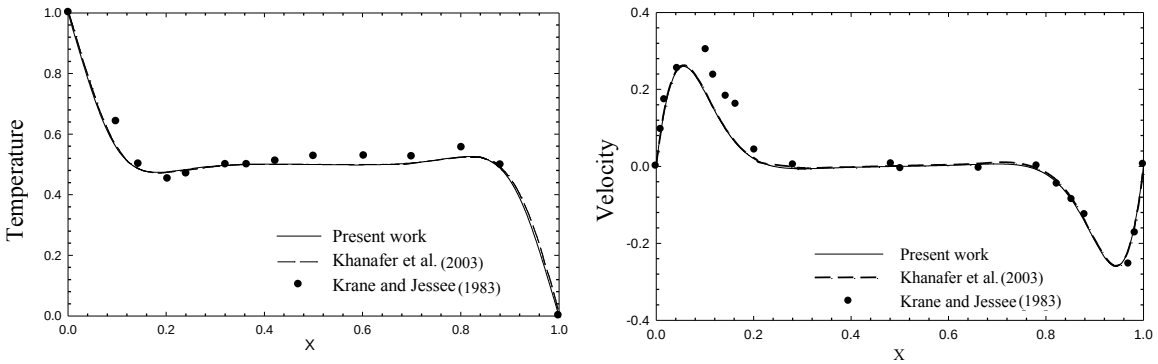

Figure 2 – Comparison of temperature velocity in y-direction at midsection ($Y = 0.5$) for square enclosure with differentially heated vertical walls for Ra = 1.89, Pr = 0.71.

Second validation is shown in Fig. 2. Temperature and velocity profiles in the y-direction are shown for the mid-section (Y=0.5). The geometry and boundary conditions are the same as the ones in the first comparison. However, Ra is 1.89 and Pr is 0.71. In this case, there are some experimental results from Krane and Jessee (1983) and numerical ones from Khanafer et al. (2003). It has an excellent agreement with the numerical values and a similar behavior with

ISSN 2176-5480

the experimental ones. The third validation (not shown here) is the same benchmark problem in the previous comparisons. This time, the temperatures on the isothermal surfaces are -1 and 1, Pr = 0.7, and Ra = 10^3, 10^4, 10^5. The temperature and v-velocity profiles are selected at Y = 0.5. The figures were contrasted with the ones presented in Khanafer et al. (2003) and Fidap (1990). The pictures were exactly superposed on paper and they agreed very well.

The last validation presented here is shown in Table 3 and it is related to nanofluid behavior. The problem is taken from Aminossadati and Ghasemi (2009). The problem consists of a square cavity with a heat source with length B placed on the middle of the bottom surface. All walls are cooled at temperature zero, but the remaining bottom surface, which is isolated. The base fluid is water with Pr = 6.2 and the nanoparticles used are Copper, Alumina and Titanium Oxide. Results for average Nusselt number and maximum temperature on the heat source are obtained for Ra equal 10^3, 10^4(not shown), 10^5(not shown) and 10^6. In general, an excellent agreement is observed.

Table 2 - Comparison for square differentially heated cavity with wall temperatures 0 and 1.

	Present	Khanafer et al. (2003)	Barakos and Mitsoulis (1994)	Markatos &Pericleous (1984)	De Vahl Davis (1962)	Fusegi et al. (1991)
$Ra=10^3$						
Nu	1.1208	1.118	1.114	1.108	1.118	1.105
Umax (at *y/H*)	0.1379 (0.8120)	0.137 (0.812)	0.153 (0.806)	- (0.832)	0.136 (0.813)	0.132 (0.833)
Vmax (at *x/H*)	0.1400 (0.1780)	0.139 (0.173)	0.155 (0.181)	- (0.168)	0.138 (0.178)	0.131 (0.200)
$Ra=10^6$						
Nu	8.8363	8.826	8.806	8.754	8.799	9.012
Umax (at *y/H*)	0.0760 (0.8500)	0.077 (0.854)	0.077 (0.859)	- (0.872)	0.079 (0.850)	0.084 (0.856)
Vmax (at *x/H*)	0.2620 (0.038)	0.262 (0.039)	0.262 (0.039)	- (0.038)	0.262 (0.038)	0.259 (0.033)

Table 3 - Comparison for the case with a heater on the bottom of a square cavity with $\emptyset = 0.1$, $B = 0.4$ and $Pr = 6.2$.

		Nu_m		T_{max}	
		Present	Aminossadati and Ghasemi (2009)	Present	Aminossadati and Ghasemi (2009)
$Ra=10^3$	*Cu*	5.4681 *(0.30%)*	5.451	0.205 *(0.00%)*	0.205
	Al_2O_3	5.4075 *(0.30%)*	5.391	0.207 *(0.00%)*	0.207
	TiO_2	5.2058 *(0.32%)*	5.189	0.215 *(0.00%)*	0.215
$Ra=10^6$	*Cu*	13.5222 *(2.53%)*	13.864	0.109 *(1.84%)*	0.107
	Al_2O_3	13.4093 *(1.89%)*	13.663	0.110 *(1.82%)*	0.108
	TiO_2	13.1595 *(1.95%)*	13.416	0.113 *(1.77%)*	0.111

4. MESH INDEPENDENCY STUDY

Two grids were studied. The grid with 51388 elements was adopted. A criterion for this choice is the CPU time suitable to run cases that are supposed to present results for extreme physical parameters such as Gr = 10^3 and Gr =10^5, and volume fraction 0 (pure water) and 0.01. A special attention is given to the elements adjacent to the wall on which the average Nusselt numbers on the heat source and cold wall, Nu_{hs} is going to be evaluated, since greater temperature gradients are expected there. The mesh quality is under the minimum angle of element internal angles, that is, elements are built by trying to set element angles as close as 90 degrees. The machine used to run all cases has 6Gb of RAM and processor Intel®Core™ 2 Duo CPU P7350 2Ghz. The convergence criterion to stop the program is:

$$Res = \frac{abs(Vel(\tau_i) - Vel(\tau_{i-1}))}{\Delta\tau} \leq 10^5 \tag{21}$$

where Res is the "largest velocity residual" in the entire domain in two consecutive time steps, that is:

ISSN 2176-5480

$$\Delta\tau = \tau_i - \tau_{i-1} = 0.0005 \tag{22}$$

The velocity field lasts more than the temperature field to achieve convergence. This is why it is used in Eq. (21).

5. RESULTS

Figure 3 shows the isotherms and streamlines for Grashof numbers 10^3, 10^4, and 10^5, and Re = 50, 100, and 500, with nanoparticle concentration PHI equal to 1%. In general, for the cases just mentioned, there are flow recirculations. They are present near the inlet, in the right lower corner, and around the heat source. Recirculations may be brought about when the flow encounters a high pressure region and it must deviate from its path to another, practically contrary to the one the flow was following. Those high pressure regions may appear when one flow "blocks" the passage of another flow. This can be clearly illustrated in the cases where the forced velocities (primary flow) are predominant, that is, when Reynolds number is 500. The nanofluid that rises due to buoyancy forces and is also influenced by the adjacent primary flow does not have power enough to cross the primary flow and exits the cavity.

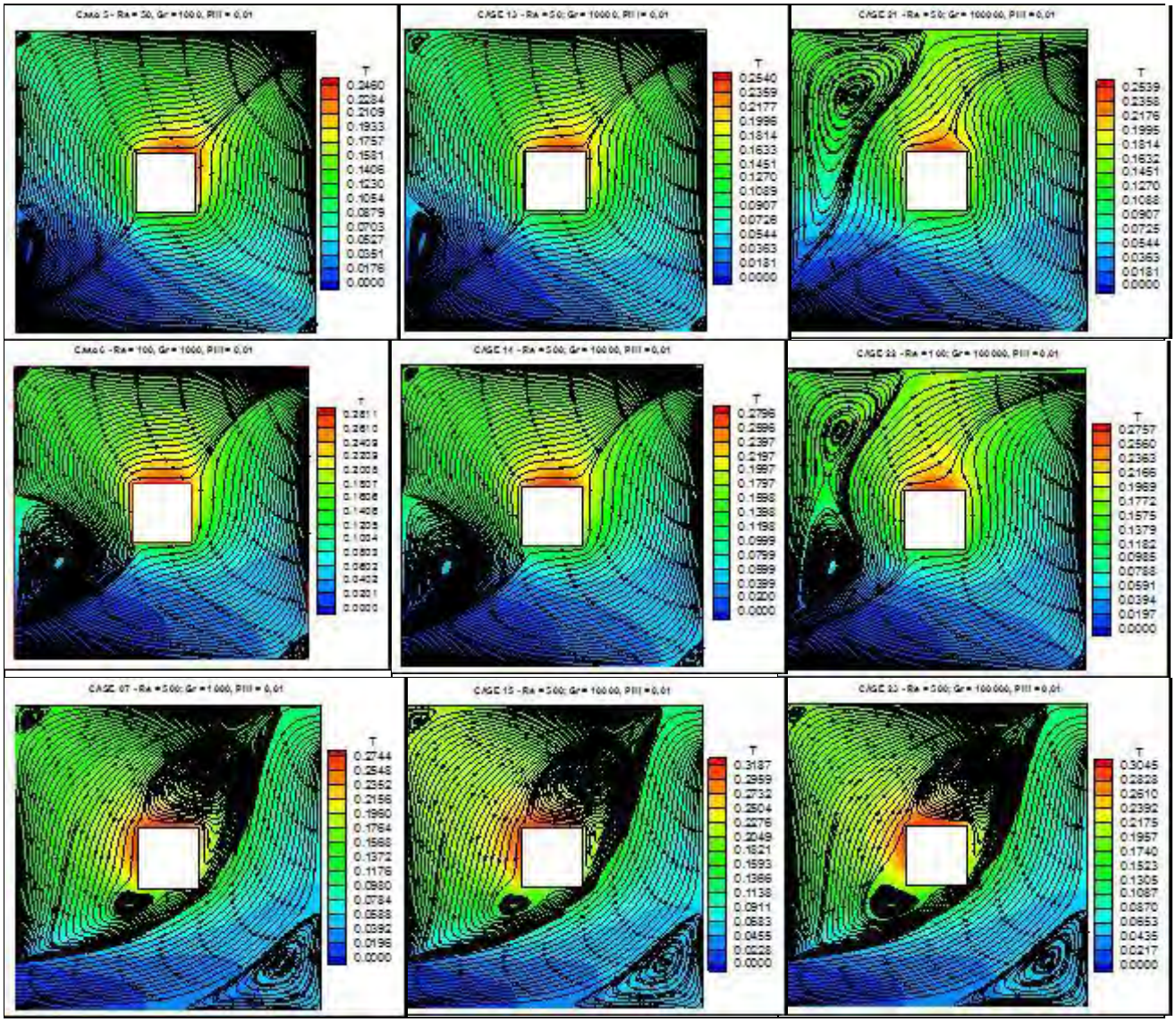

Figure 3. Isotherms and streamlines for cases with Gr = 10^3, 10^4, and 10^5, and Re = 50, 100, and 500, PHI = 0.1

This creates secondary and also tertiary flows that are stuck around the heater and, therefore, creating an overheated region. One can observe from cases that go from left to right and from top to bottom in the table, the overheated flow region near the heat source goes from right to left on the top surface of the heated module. This is related to what extent the primary flow that starts from the inlet, goes towards the outlet by passing below the heat source, gets stronger. The

ISSN 2176-5480

stronger the primary flow is, the more difficult it is for the flow to cross that forced velocity path. Maybe, this is not the best layout to be followed. If the manufacturer of a heat exchanger has the opportunity to change the layout, maybe the one which brings forced convection downstairs against the ascending buoyancy forces may present a certain enhancement. But of course, this is some expectations and, hence, studies must be carried out to estimate any conclusion. Anyway, this is food for thought for future work. By keeping Grashof number constant (cases for Gr = 10^4 and 10^5), the temperature on the heat source surface increases when increasing the forced velocity at the inlet. Generally, one expects the heat transfer to increase when increasing Reynolds number. This happens almost in every paper we find in literature. However, here it is just proven that it may be not true. For Gr = 10^4, the maximum temperature goes from 0.240 to 0.3187 as Re is ranged from 50 to 500. Also, for Gr = 10^5, the maximum temperature goes from 0.2539 to 0.3045 for the same Re range. Thus, geometry together with boundary conditions may bring contradictions to what the reader is accustomed to face.

Figure 4 denotes the heat transfer behavior related to the ratio of inertia forces to viscous forces represented by the Reynolds number. For all cases, the heat transfer does not increase with Re due to reasons about which they were commented on previously in the isotherm and streamline figure section. Nevertheless, although the heat transfer enhancement is of low order, the nanoparticle concentration appears to increase heat transfer for PHI = 1%. This is not true for Gr = 10^4 and Re = 500. The high thermal conductivity of copper is expected to augment heat transfer; however more studies must be carried out to evaluate such case when Gr = 10^4 and Re = 500. As the method takes into consideration the Petrov-Galerkin method and the penalty formulation, it is suggested for next work that mass and energy conservation in the whole cavity, especially for that case, must be thoroughly analyzed.

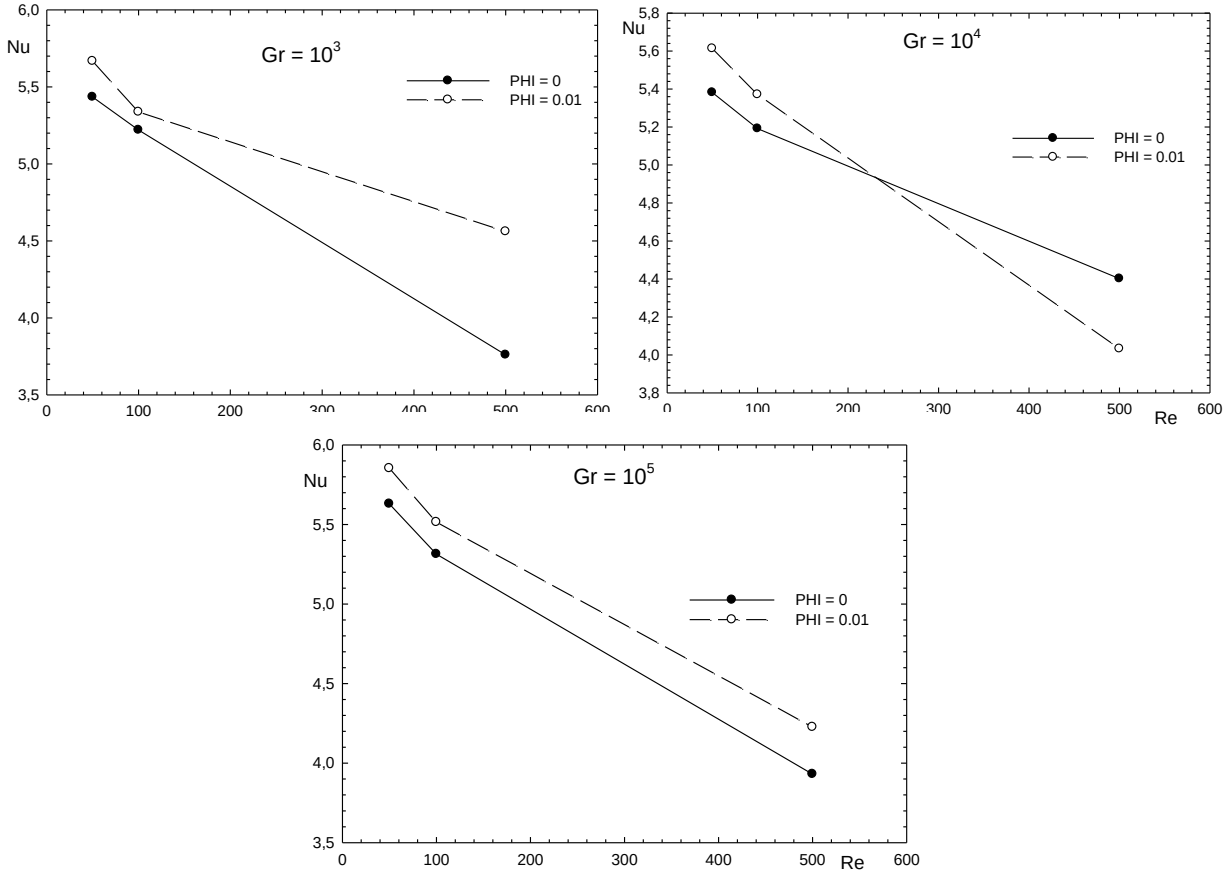

Figure 4 – Nusselt versus Reynolds number for Gr = 10^3, 10^4 and 10^5 for PHI = 0 and 1%.

ISSN 2176-5480

Table 1 – Values of T_{max} on the heat module and Nusselt number for pure water and PHI = 1%.

Case	Re	Gr	Nusselt	T_{MAX}	Case	Nusselt	T_{MAX}
			PHI = 0			PHI = 0.01	
1	50	10^3	5.4342	0.255	5	5.6665 4%	0.246 -4%
2	100	10^3	5.2194	0.2849	6	5.3369 2%	0.2811 -1%
9	50	10^4	5.3822	0.2639	13	5.6133 4%	0.254 -4%
10	100	10^4	5.1920	0.2973	14	5.3711 3%	0.2796 -6%
17	50	10^5	5.6288	0.2632	21	5.8528 4%	0.2539 -4%
18	100	10^5	5.3130	0.2846	22	5.5139 4%	0.2757 -3%

Finally, table 1 shows some values of Nusselt number and the maximum temperature on the heat source surface for the two nanoparticle concentrations covered, that is, PHI = 0 and 1%. In general, the heat transfer and the maximum temperature enhancements on the heat source, where the heat module cooling is aimed, are the order of 4%. Although this order is not high, it may sound very interesting when it is then thought in terms of heat exchanger performance and manufacturing.

6. CONCLUSIONS

The heat transfer is studied in a square ventilated cavity with a heat source inside the cavity. The work fluid is a Cu/water nanofluid considering two nanoparticle concentrations. Reynolds number was varied from 50 to 500 and the Grashof number from 10^3 to 10^5. The direction of the inlet towards the outlet flow was in favor of buoyancy forces, that is, upwards direction. Although the forced velocities were in the ascending direction, this work presented an interesting result when the Reynolds number is increased by keeping the Grashof number constant. One should have expected expect from this that heat transfer should have increased with Reynolds going up. Nevertheless, the opposite happened. This occurred due to a series of combined factors: the geometry and also the velocities involved. As Re was increased, so was the strength and size of the recirculation around the heat source and therefore impairing colder fluid to reach the heat source. The fluid was stuck around the heated source because it did not have strength enough to break the high pressure region caused by the primary flow due to forced velocities towards the exit. In general, the nanoparticle concentration effect of heat transfer enhancement was the order of 4% for both cases, that is, concentrations of 0 (pure water) and 1%. The authors strongly recommend that for high Re that mass and energy must be more thoroughly studied for the parameters considered in this study.

7. ACKNOWLEDGEMENTS

The authors thank CAPES because the code was developed when the first author was taking a post-doctoral course in the USA, Fapemig because an academic research student is involved, and, finally, CNPq once some code developments were carried out when the first author had its scholarship.

8. REFERENCES

Aminossadati S. M., Ghasemi B., 2009. “Natural convection cooling of a localized heat source at the bottom of a nanofluid-filled enclosure”, *European Journal of Mechanics B/Fluids*, Vol. 28, p. 630-640.

Arefmanesh A. and Mostafa M., 2011. “Effects of uncertainties of viscosity models for Al_2O_3-water nanofluid on mixed convection numerical simulations”, *International Journal of Thermal Sciences*, Vol. 50, p. 1706-1719.

Arquis E., Rady M. A.; Nada A. S., 2007. “A numerical investigation and parametric study of cooling an array of multiple protruding heat sources by a laminar slot air jet”, *International Journal of Heat and Fluid Fl*ow, Vol. 28, p. 787–805.

Barakos G., Mitsoulis E., 1994. “Natural convection flow in a square cavity revisited: laminar and turbulent models with wall functions”, *International Journal of Numerical Methods in Fluids*, Vol. 18, p. 695-719.

Brinkman H. C., 1952. “The viscosity of concentrated suspensions and solution”, *Journal of Chemical Physics, Vol.* 20, p. 571-581.

De Val Davis, 1962. “Natural convection of air in a square cavity, a benchmark numerical solution”, *International*

ISSN 2176-5480

Journal of Numerical Methods in Fluids, Vol. 3, p. 249-264.

Fusegi T., Hyun J. M., Kuwahara K., Farouk B., 1991. "*A numerical study of three-dimensional natural convection in a differentially heated cubical enclosure*", International Journal of Heat and Mass Transfer, Vol. 34, p. 1543-1557.

FIDAP Theoretical Manual, Fluid Dynamics International, Evanston, IL, USA, 1990.

Ho C. J., Chen M. W., Li Z. W., 2008. "Numerical simulation of natural convection of nanofluid in a square enclosure: effects due to uncertainties of viscosity and thermal conductivity", *International Journal of Heat and Mass Transfer,* Vol. 51 (17-18), p. 4506-4516

Khanafer K., Vafai K., Lightstone M., 2003. "Buoyancy-driven heat transfer enhancement in a two-dimensional enclosure utilizing nanofluids", *International Journal of Heat and Mass Transfer*, Vol. 46, p. 3639-3653.

Krane R. J., Jessee J., 1983. "Some detailed field measurements for a natural convection flow in a vertical square enclosure", *Proceedings of the First ASME-JSME Thermal Engineering Joint Conference*, Vol. 1, p. 323-329.

J. Jung, H. Oh, H. Kwak, 2009. "Forced convective heat transfer of nanofluids in microchannels", International Journal of Heat and Mass Transfer, Vol. 52, p. 466-472.

Maxwell J., A treatise on electricity and magnetism, second ed. Oxford University Press, Cambridge, UK, 1904.

Madhusudhana Rao G. & Narasimham G. S. V. L., 2007. Laminar conjugate mixed convection in a vertical channel with heat generating components, International Journal of Heat and Mass Transfer, Vol. 50, p. 3561–3574.

Markatos N. C., Pericleous K. A., 1984. "Laminar and turbulent natural convection in an enclosed cavity", *International Journal of Heat and Mass Transfer*, Vol. 27, p.772-775.

Nassan T. H., Heris S. Z., Noie S. H., 2010. "*A comparison of experimental heat transfer characteristics for Al_2O_3/water and CuO/water nanofluids in square cross-section duct*", International Communications of Heat and Mass Transfer, Vol. 37, p. 924-928.

Oztop H. F., Abu-Nada E., 2008. "Numerical study of natural convection in partially heated rectangular enclosures filled with nanofluids", *International Journal of Heat and Fluid Flow*, Vol. 29 (5), p. 1326-1336.

Rostamani M., Hosseinizadeh S. F., Gorji M., Khodadadi J. M., 2010. "Numerical study of turbulent forced convection flow of nanofluids in a long horizontal duct considering variable properties", *International Communications in Heat and Mass Transfer*, Vol. 37 (10), p. 1426-1431.

Shahi M., Mahmoudi A. H., Talebi F., 2010. "Numerical study of mixed convective cooling in a square cavity ventilated and partially heated from the below utilizing nanofluid", *International Communications in Heat and Mass Transfer,* Vol. 37, p. 201-213.

9. RESPONSIBILITY NOTICE

The authors are the only responsible for the printed material included in this paper.